Synthesis, Structure, and Properties of Biimidazole-Chelated Arylruthenium Complexes

Bikash Kumar Panda,[a] Suman Sengupta,[a] and Animesh Chakravorty*[a,b]

Keywords: Ruthenium / Fluorescence / Marcocyclic ligands / Hydrogen bonding

By reacting Ru(η^2-RL)(PPh_3)$_2$(CO)Cl (**1**) with excess 4,5-dimethyl-2,2′-biimidazole (dmbi), organometallics of the type [Ru(η^1-RL)(PPh_3)$_2$(CO)(dmbi)](PF_6) (**2**) have been isolated in excellent yield (η^2-RL is C_6H_2O-2-CHNHC_6H_4R(*p*)-3-Me-5, η^1-RL is C_6H_2OH-2-CHNC_6H_4R(*p*)-3-Me-5 and R is Me, OMe and Cl). In this process the dmbi ligand undergoes five-membered chelation, the iminium-phenolato function tautomerizes to the imine-phenol function and the Schiff base performs a large rotation around the Ru–C bond. The crystal and molecular structure of [Ru(η^1-MeL)(PPh_3)$_2$(CO)(dmbi)](PF_6)·CH_2Cl_2 is reported. For steric reasons the carbon monoxide ligand is located *syn* to the phenolic oxygen atom as opposed to *anti* in the precursor **1**. In the hydrogen bonded imine-phenol function the O–H, H···N, and N···O distances are 0.83(8), 1.77(8), and 2.552(6) Å, respectively, the O–H···N angle being 156(2)°. The Ru(dmbi) chelate along with the metallated carbon atom and the CO ligand define an equatorial plane from which the metallated aldimine fragment is rotated by 34.5° due to interligand repulsion. This results in two unequal [2.348(2) and 2.411(2) Å] Ru–P bonds and an apparent suppression of the *trans* influence of the metallated carbanionic site. The cation and anion in the complex are engaged in N–H···F and C–H···F hydrogen bonding, generating a centrosymmetric dimer in the lattice. One of the hydrogen bonds, characterized by H···F, 2.03(8) Å and N–H···F, 166(2)°, is particularly strong. Solutions of **2** absorb near 400 nm and emit near 460 nm with quantum yields and lifetimes of ca. 10^{-3} and ≤ 20 ns, respectively. The emission, which probably involves the ^{3}MLCT state incorporating a π^*(dmbi) contribution, is peculiar to the coligation of η^1-RL and dmbi to bivalent ruthenium. In dichloromethane solution **2** displays a quasireversible $\mathbf{2}^+/\mathbf{2}$ couple near 0.70 V vs. SCE [$\mathbf{2}^+$ is the ruthenium(III) analogue of **2**]. Coulometrically generated solutions of $\mathbf{2}^+$ display a strong absorption near 400 nm and rhombic EPR spectra with *g* values near 2.55, 2.15, and 1.83.

Introduction

New orthometallated ruthenium compounds are of current interest in terms of synthesis[1−3] reactivity[1,4−9] and photophysical properties.[10,11]

The decarbonylative metallation of 4-methyl-2,6-diformylphenol by $Ru(PPh_3)_3Cl_2$ in the presence of primary aromatic amines ($RC_6H_4NH_2$) furnishes organoruthenium species of the type Ru(η^2-RL)(PPh_3)$_2$(CO)Cl, (**1**), incorporating a four-membered chelate ring adjacent to a hydrogen-bonded iminium-phenolato ring.[12−14] The reactivity of **1** is under our scrutiny. Alkynes and isocyanides promote metallacycle expansion[5,6,8,15,16] but bidentate monoanionic σ-donor reagents such as carboxylates, nitrate, nitrite, xanthate, and pyridine-2-thiolate invariably form a four-membered chelate ring.[17−20]

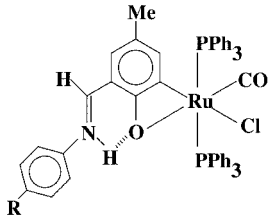

1

The richness of this reaction chemistry prompted us to explore the treatment of **1** with an electroneutral heterocyclic ligand suited for five-membered *N*,*N*-chelation − with the result that 4,5-dimethyl-2,2′-biimidazole (dmbi) has been used to afford a crystalline organoruthenium system, characterized by hydrogen bonding interactions within itself and with anions in the lattice. This is accompanied by changes in the rotameric and tautomeric states of the Schiff base ligand. The structure and properties of the new organometallics, which are also luminescent in the visible region, are scrutinized here.

Results and Discussion

Reaction of 1 with dmbi: Chelation and Tautomerization

Addition of excess dmbi to a violet solution of Ru(η^2-RL)(PPh_3)$_2$(CO)Cl (**1**) in boiling $MeOH/CH_2Cl_2$ solution

[a] Department of Inorganic Chemistry, Indian Association for the Cultivation of Science,
Kolkata 700032, India
Fax: (internat.) +91-(0)33-2473-2805
E-mail: icac@mahendra.iacs.res.in
[b] Jawaharlal Nehru Centre for Advanced Scientific Research, Bangalore 560 064, India

  DOI: 10.1002/ejic.200300293

in the presence of NH_4PF_6 afforded the yellow salt [Ru(η^1-RL)(PPh_3)$_2$(CO)(dmbi)](PF_6) (**2**) according to Equation (1).

$$\mathbf{1} + \text{dmbi} + PF_6^- \rightarrow \mathbf{2} + Cl^- \quad (1)$$

In this work R = Me, OMe, and Cl, and specific compounds are identified with R in parenthesis, e.g. for **2** (Me) R = Me. Ruthenium complexes of biimidazoles have received some attention[21−25] but organoruthenium species incorporating chelation by such ligands as in **2** appear to be unprecedented. The salt **2** has been uniformly isolated in pure form in >80% yield. An isomer (the coordinating nitrogen atoms interchanged) of **2** is possible in principle but it has never been observed. Careful examination of ^{1}H NMR spectra of crude samples (before recrystallization) did not reveal any extra methyl or other signals apart from those characterizing **2** (see Exp. Sect.).

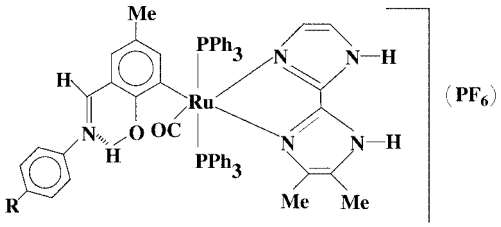

2

In Equation (1) the Ru−Cl and Ru−O (phenolato) bonds are displaced by the chelating dmbi ligand. With the liberation of the phenolato oxygen, the Schiff base fragment assumes the imine-phenol tautomeric form **3**, as opposed to the zwitterionic iminium-phenolato form **4** present in **1**.[12] This has been proven by structure determination (vide infra) and is fully consistent with spectroscopic data.

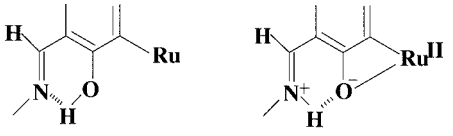

3 **4**

Thus the C=N stretching frequency in **2** is significantly lower at ca. 1600 cm^{-1} than that in **1** (ca. 1620 cm^{-1}), as expected.[26,27] Also, the aldimine CH signal in ^{1}H NMR in **2** is at a lower field, ca. 8.0 ppm as compared to ca. 7.5 ppm in **1**. The O−H resonance in **2** is a relatively sharp signal near 13 ppm, having a half-height width of ca. 30 Hz. In contrast the iminium N−H resonance in **1** is broad (width, ca. 150 Hz) due to the quadrupole moment of the nitrogen atom.[12] The prototropic transformation between **1** and **2** has certain similarities with the imine−iminium tautomerization in rhodopsins.[26]

Equation (1) is believed to proceed[17,28] via *cis* attack of chloride/O(phenolato) by dmbi as stylized in **5**. The anchored ligand can then displace both chloride and phenolato oxygen atom to achieve chelation as in **6** with concomitant prototropic and rotameric (vide infra) changes.

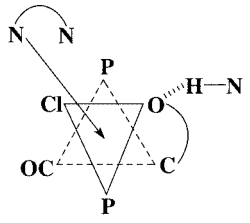

5

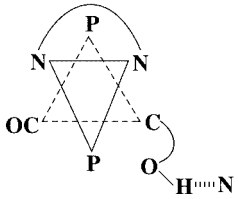

6

Characterization

Type **2** organometallics are diamagnetic (Ru^{II}, idealized t_{2g}^6) and behave as 1:1 electrolytes in acetone solution (Λ, 133−138 Ω^{-1} cm^2 mol^{-1}). The C≡O stretching frequency (ca. 1940 cm^{-1}) in **2** is indicative of dπ(Ru)−pπ(dmbi) back-bonding. In **1** as well as in the acetate and other derivatives this stretch lies systematically at lower frequencies, near 1920 cm^{-1}.[12,17−20]

In the ^{1}H NMR spectra the 3-H and 5-H proton signals of the metallated ring are sharp singlets near 6.5 ppm. The C(4)-Me signals near δ = 1.8 ppm are subject to shielding by phosphane phenyl rings.[12,17,29] The same applies to the C(22)-Me signal near 1.7 ppm; the C(21)-Me resonance is near 2.0 ppm. The PPh_3, Schiff base (C_6H_4R), and the biimidazole aromatic proton signals form a complex multiplet in the region 6.8−7.4 ppm. The dmbi N−H protons resonate near 10.2 ppm. The chemical shifts of the imine-phenol protons are considered above. The photophysical and redox properties of the complexes are examined below.

Structure: Nonbonded Interactions, Rotameric Change, and Hydrogen Bonding

The dichloromethane solvate [Ru(η^1-MeL)(PPh_3)$_2$(CO)-(dmbi)](PF_6)·CH_2Cl_2, afforded crystals suitable for structure determination. A view of the cation (Figure 1) and

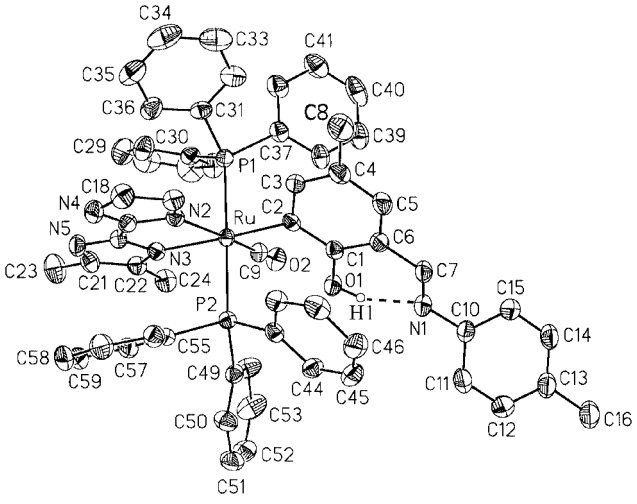

Figure 1. Perspective view and atom labeling scheme for the cation of **2**(Me)·CH_2Cl_2. All non-hydrogen atoms are represented by 30% thermal probability ellipsoids.

Table 1. Selected bond lengths (Å) and angles (°) for complex **2**(Me)·CH_2Cl_2

Bond lengths			
Ru−P(1)	2.348(2)	Ru−N(3)	2.157(4)
Ru−P(2)	2.411(2)	C(9)−O(2)	1.152(6)
Ru−C(2)	2.068(5)	C(7)−N(1)	1.259(7)
Ru−C(9)	1.791(5)	C(1)−O(1)	1.347(6)
Ru−N(2)	2.166(4)	N(1)···O(1)	2.552(6)
Angles			
P(1)−Ru−P(2)	175.7(1)	P(2)−Ru−C(2)	87.9(1)
P(1)−Ru−N(2)	91.0(1)	Ru−C(9)−O(2)	174.8(5)
P(1)−Ru−N(3)	90.8(1)	C(2)−Ru−N(2)	95.4(2)
P(1)−Ru−C(9)	87.0(2)	C(9)−Ru−N(3)	96.5(2)
P(1)−Ru−C(2)	90.5(1)	C(9)−Ru−N(2)	172.4(2)
P(2)−Ru−N(2)	85.2(1)	N(2)−Ru−N(3)	76.3(2)
P(2)−Ru−N(3)	90.3(1)	C(9)−Ru−C(2)	91.9(2)
P(2)−Ru−C(9)	97.1(2)		

selected bond parameters (Table 1) are given here. All the hydrogen atoms in the structure, except those of CH_2Cl_2, were directly observable in difference Fourier maps, which helped in characterizing the hydrogen bonds, vide infra. In Figure 1 only the phenolic hydrogen is explicitly shown. The solvent of crystallization CH_2Cl_2 displays a nonbonded Cl···Cl interaction [3.576(4) Å] with another symmetry related CH_2Cl_2 molecule, the two forming a centrosymmetric pair in the lattice.

The $RuC_2P_2N_2$ coordination sphere has a severely distorted octahedral geometry. The angles subtended by *cis* and *trans* pairs of ligands span the ranges 76−98° and 171−176°, respectively. On the basis of covalent radii, the idealized Ru^{II}−C(sp^2) bond length is estimated to be 2.06 Å.[17,30] The observed Ru−C(2) is 2.068(5) Å. The Ru−N(3) bond is not lengthened by the *trans* influence of the carbanionic C(2) site due to certain repulsive interactions in the structure, see below.

The Ru(dmbi) chelate fragment (excluding the methyl groups) along with the metallated carbon atom C(2) and the carbon monoxide ligand constitute a satisfactory plane of mean deviation 0.03 Å (plane A). Another relevant plane (plane B) is the metallated aldimine ring defined by Ru, C(1) to C(8), N(1), O(1) (mean deviation 0.03 Å). The two planes are noncoplanar as highlighted in **7**, the dihedral angle between them is 34.5°. As a result the environment is more crowded around P(2), and Ru−P(2) [2.411(2) Å] is significantly longer than Ru−P(1) [2.348(2) Å]. In the precursor complex **1** the Schiff base lies on the equatorial plane and the two Ru−P lengths are both 2.387(2) Å.[12]

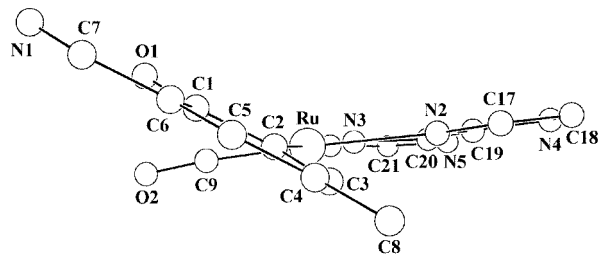

7

The noncoplanarity of A and B planes arise from the repulsive nonbonded interactions between the dmbi and Schiff base ligands. Thus C(17)···C(3) [3.298(7) Å] is less than the sum (3.40 Å) of the van der Waals (vdW) radii of the two carbon atoms.[31] The distance would have been even lower, further augmenting the repulsion, if the A and B planes were coplanar. The repulsive interaction is also expressed in an effective lengthening of the Ru−N(2) bond. The *trans* influence of the carbanionic C(2) site should normally make the Ru−N(3) bond longer than the Ru−N(2) bond although the electron-donating methyl group adjacent to N(3) may marginally counter this effect. In practice the two bond lengths − 2.157(4) and 2.166(4) Å, respectively − are equal within experimental error, primarily due to the nonbonded repulsion noted above.

The conversion of **1** into **2** is attended by a large rotation of the Schiff base fragment around the Ru−C(2) bond. The carbon monoxide ligand lies *syn* to the metallated carbon atom in both **1** and **2** but it is respectively *syn* and *anti* to the phenolic C−O function in **2** and **1**.[12] The O(1)−C(1)···C(9)−O(2) torsion angle in **2**(Me)·CH_2Cl_2 is 46.7°. The computer-generated hypothetical *anti* configuration of dmbi fragment is shown in **8** where the estimated C(17)···O(1) and N(2)···O(1) are 2.416(5) Å and 2.621(6) Å, respectively, are far below the respective sums of the vdW radii (3.20 and 3.05 Å).[31] The *anti* configuration is thus unstable and the above-noted conformational change occurs to relieve the strain. The observed C(17)···O(1) and N(2)···O(1) distances in the *syn*-configured complex are 5.660(5) and 4.930(6) Å, respectively.

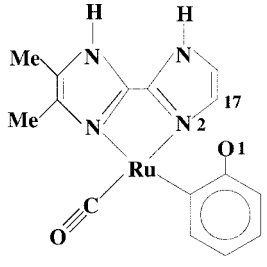

8

Within the imine-phenol fragment of **8**, O−H, H···N, and N···O are 0.83(8), 1.77(8), and 2.552(6) Å respectively, the O−H···N is 156(2)°. The hydrogen bonding is thus very unsymmetrical. In the iminium-phenolato fragment **4** of the precursor **1** the relevant bond lengths and angle are: N−H, 0.99(6) Å, H···O, 1.75(5) Å, N···O, 2.665(12) Å, and N−H···O, 144(1)°.[12] In effect, the hydrogen bonding is stronger (shorter N···O distance) in the imine-phenol species.

The dmbi ligand in the cation and the PF_6^- anion are engaged in N−H···F and C−H···F hydrogen bonding. The

centrosymmetric dimer thus generated is shown in Figure 2 along with approximate bond parameters. In organometallic hexafluorophosphate salts, H···F distances <2.6 Å, along with X−H···F (X = C, N, O) angles >90°, generally indicate significant hydrogen bonding.[32] Of the three hydrogen bond types in Figure 3 the, N(5)−H···F(1) bond is particularly strong [H···F, 2.03(8) Å; N−H···F, 166(2)°].

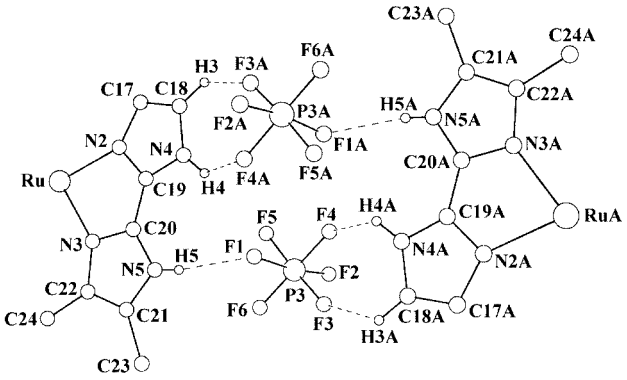

Figure 2. Hydrogen bonding in crystals of **2**(Me)·CH_2Cl_2. Relevant bond lengths (Å) and angles (°) are N(5)···F(1), 2.775(5); H(5)···F(1), 2.03(8); N(4)···F(4), 2.945(5); H(4)···F(4), 2.31(9); C(18)···F(3), 3.144(6); H(18)···F(3), 2.54(7). N(5)−H(5)···F(1), 166(2); N(4)−H(4)···F(4), 131(3); C(18)−H(18)···F(3), 123(1)

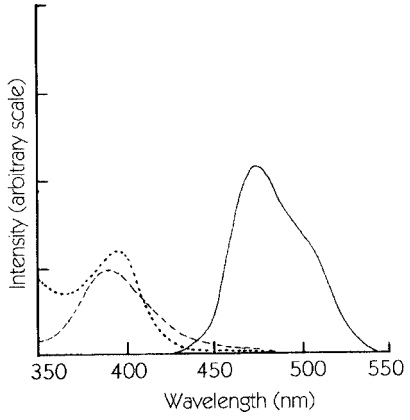

Figure 3. Absorption (···) fluorescence (——) and excitation (− − −) spectra of **2**(Cl) in dichloromethane solution.

Photophysical Properties

Type **2** complexes display two allowed transitions near 320 and 400 nm (Table 2). The later band is weaker in intensity and is believed to have significant dπ(Ru)−π*(dmbi) MLCT character. Dichloromethane solutions of **2** are fluorescent at room temperature, the emission peak lying near 460 nm. The quantum yields (φ_r) are nearly one order of magnitude lower than that of the $[Ru(bpy)_3]^{2+}$ standard[33] (Table 2).

Excitation spectral studies have revealed that the emission is associated with the absorption band near 400 nm. A representative case is shown in Figure 3. Assuming that the band has MLCT character, as suggested above, the possible involvement of the ^{3}MLCT state incorporating a π*(dmbi) contribution is implicated in the emission process. However, tris-biimidazole complexes of bivalent ruthenium are nonemitters at room temperature.[21,34] Further the parent type **1** organometallics also do not emit in the visible region. Thus the observed emission in **2** is a property peculiar to the coligation of η^1-RL and dmbi to bivalent ruthenium. Lifetime studies revealed single-exponential decay with $\tau_0 \leq 20$ ns, which is shorter than the usual (10^2-10^3 ns) lifetimes of fluorescent ruthenium(II) complexes of conjugated nitrogenous ligands.[21,23]

Electrochemistry: Metal Oxidation

In dichloromethane solution **2** displays a quasireversible (peak-to-peak separation, ca. 100 mV) cyclic voltammetric response assigned to the couple of Equation (2) where $\mathbf{2}^+$ represents the ruthenium(III) analogue of **2**.

$$\mathbf{2}^+ + e \rightarrow \mathbf{2} \quad (2)$$

The reduction potentials ($E_{1/2}$) lie near 0.70 V vs. SCE and become more positive as the electron-withdrawing power of the R group increases (OMe < Me < Cl), see Table 2. The one-electron nature of the couple is consistent with current height data, as compared to those of the one-electron standard $[Ru(bpy)_3]^{2+}$. More importantly exhaustive coulometric oxidation at 0.9 V afforded a coulomb count corresponding to a one-electron transfer (Table 2).

The trivalent organometallics $\mathbf{2}^+$, generated coulometrically, have been examined in solution. Their cyclic voltammograms (initial scan cathodic) are virtually superimposable on those of **2** (initial scan anodic), showing that $\mathbf{2}^+$ retains the gross structure of **2**. Orange-red solutions of $\mathbf{2}^+$ are characterized by an intense band near 400 nm, associ-

Table 2. Spectral and electrochemical data of **2**

Complexes	UV/Vis data[a] λ_{max}, nm (ε,[b] $M^{-1}cm^{-1}$)	Emission data λ_{max}, nm (φ_r)[a] [c]	Electrochemical data $E_{1/2}$, V (ΔE_p, mV)[d]	n[e]
2(Me)	320 (20970), 390 (4680)	464 (5.6×10^{-3})	0.69 (130)	1.07
2(OMe)	322 (23700), 394 (5210)	461 (3.0×10^{-3})	0.65 (85)	1.03
2(Cl)	321 (22760), 397 (4470)	467 (5.3×10^{-3})	0.71 (95)	0.98

[a] Solvent is dichloromethane. [b] Molar absorption coefficient. [c] Excitation at the higher wavelength absorption peak. [d] Solvent is dichloromethane; ΔE_p is peak-to-peak separation. [e] $n = Q/Q'$ where Q is the observed coulomb count and Q' is the calculated coulomb count for one-electron transfer.

Table 3. Electronic and EPR spectroscopic data of $\mathbf{2}^+$

Complexes	UV/Vis data[a] λ_{max}, nm (ε,[b] $M^{-1}cm^{-1}$)	EPR g values[c] g_1	g_2	g_3
$\mathbf{2}(Me)^+$	324 (356560), 397(26710), 518 (4830)	2.528	2.141	1.818
$\mathbf{2}(OMe)^+$	319 (34960), 401 (24410), 512 (2530)	2.553	2.158	1.818
$\mathbf{2}(Cl)^+$	321 (37950), 403 (27710), 515 (3500)	2.578	2.159	1.856

[a] Solvent is dichloromethane. [b] Molar absorption coefficient. [c] In 1:1 dichloromethane/toluene frozen glass (77 K).

ated with a shoulder near 520 nm (Table 3). The solutions are EPR-active when frozen into the glassy state (dichloromethane/toluene, 77 K), giving rise to well-resolved rhombic spectra that are consistent with a low-spin $4d^5$ configuration in a nonaxial geometry.[35,36] A representative spectrum (Figure 4) and the g values (Table 3) are given here.

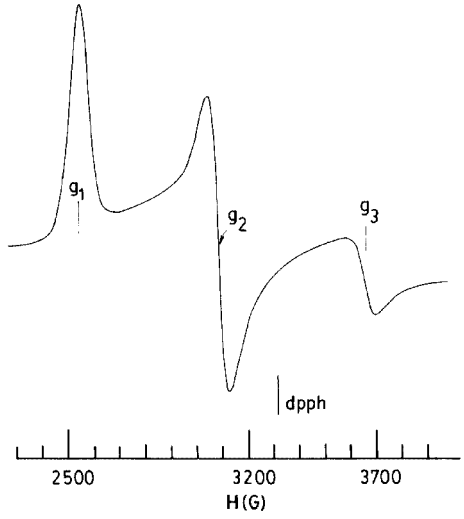

Figure 4. X-band EPR spectrum of electrogenerated $\mathbf{2}(OMe)^+$ in dichloromethane/toluene glass at 77 K. Instrument settings: power, 30 dB; modulation, 100 kHz; sweep centre, 3200 G.

Conclusions

Organometallics of type **1** are transformed into salts of type **2** upon reacting with dmbi. The conversion is attended by five-membered dmbi chelation, iminium-phenolato → imine-phenol prototropic shift and rotameric isomerization (*anti*→ *syn*) of the phenolic function with respect to the carbon monoxide ligand. The metallated aromatic ring is turned away from the dmbi chelate plane due to steric repulsion, resulting in significant inequality of the two Ru−P bonds. Also, the carbanionic *trans* influence is apparently suppressed. In solution **2** is emissive in the visible region and is electrooxidizable to its ruthenium(III) analogue $\mathbf{2}^+$, which is characterized by rhombic EPR spectra.

Experimental Section

Materials: $Ru(PPh_3)_3Cl_2$ [37] and $Ru(\eta^2\text{-RL})(PPh_3)_2(CO)Cl$[12] were prepared by reported methods, and 4,5-dimethyl-2,2′-biimidazole was obtained from Aldrich. Dichloromethane was purified for electrochemical work as described before.[35,38] All other chemicals and solvents were of analytical grade and were used as received.

Physical Measurements: Electronic and IR spectra were recorded with a Shimadzu UV-1601 PC spectrophotometer and a Nicolet Magna IR series II spectrometer respectively. ^1H NMR spectra were obtained using a Bruker 300 MHz FT NMR spectrometer. The numbering scheme used for ^1H NMR is the same as in the crystallography. Spin−spin structures are abbreviated as: s, singlet; d, doublet; t, triplet; m, multiplet. EPR spectra were recorded on a Varian E-109C X-band spectrometer fitted with a quartz dewar. Microanalyses (C, H, N) were performed using a Perkin−Elmer 240C elemental analyzer. Solution electrical conductivity was measured in acetone with a Phillips PR 9500 bridge by using a platinized electrode (cell constant of 1.05). The electrochemical measurements were performed at a platinum electrode under a nitrogen atmosphere in dichloromethane solution by using a model 620A electrochemical analyzer of CH Instruments. The supporting electrolyte was tetraethylammonium perchlorate and potentials are referenced to the saturated calomel electrode (SCE). For EPR studies $\mathbf{2}^+$ was generated coulometrically in dichloromethane solution to which dry toluene was added before freezing into the glassy state.

Fluorescence and quantum yields (using $[Ru(bpy)_3]^{2+}$ as standard,[33] $\varphi = 0.042$) were recorded with a Perkin−Elmer model LS 55 luminescence spectrometer. Luminescence lifetimes were measured in an Applied Photophysics SP-70 nanosecond fluorescence spectrometer based on a time-correlated single-photon counting technique. The decay curves were deconvoluted using the Global Fluorescence Analysis version 1.2 software of Photon Technology International.

Synthesis of Complexes: The $[Ru(\eta^1\text{-RL})(PPh_3)_2(CO)(dmbi)](PF_6)$ (**2**) complexes were synthesized in excellent yield (ca. 85%) by reacting $Ru(\eta^2\text{-RL})(PPh_3)_2(CO)Cl$ (**1**) with excess 4,5-dimethyl-2,2′-biimidazole. Details of a representative case are given below. The other compounds were prepared analogously.

2(Me): dmbi (89 mg, 0.549 mmol) was added to a hot solution of **1**(Me) (100 mg, 0.109 mmol) in a mixture of methanol (20 mL) and dichloromethane (10 mL). On subsequent heating to reflux for 3 h, the mixture changed from violet to yellow. NH_4PF_6 (30 mg, 0.184 mmol) was then added and the resultant solution was further boiled under reflux for 20 min. The solvent was then evaporated under reduced pressure and the yellow solid thus obtained was washed thoroughly with water (for removal of excess NH_4PF_6), dried, and then dissolved in dichloromethane (excess dmbi remains insoluble). The filtered solution was then stripped of solvent under reduced pressure and the residue was recrystallized from a dichloromethane/hexane (1:3) mixture followed by drying in vacuo to furnish the complex in nonsolvated form. Yield: 110 mg (85%). $C_{60}H_{54}F_6N_5O_2P_3Ru$ (1185.10): calcd. C 60.81, H 4.59, N 5.91; found C 60.75, H 4.63, N 5.85. IR (KBr): $\tilde{\nu}$ = 1939 cm^{-1}(ν_{CO}), 1591 ($\nu_{C=N}$), 847 (ν_{PF6}). ^1H NMR (300 MHz, $CDCl_3$, 298 K): δ = 12.96 (s, 1 H, O−H), 10.30 (s, 1 H, N−H), 10.20 (s, 1 H, N−H), 7.96 (s, 1 H, H7), 6.59 (s, 1 H, H5), 6.52 (s, 1 H, H3), 2.37 (s, 3 H, 13-Me), 2.02 (s, 3 H, 21-Me), 1.84 (s, 3 H, 4-Me), 1.72 (s, 3 H, 22-Me), 6.90−7.25 (m, 36 H, $2PPh_3$, H11, H12, H14, H15, H17, H18). Λ_M = 133 $\Omega^{-1}cm^2mol^{-1}$.

2(OMe): **1**(OMe) (100 mg, 0.107 mmol) and dmbi (87 mg, 0.536 mmol) were employed. Yield: 106 mg (82%). $C_{60}H_{54}F_6N_5O_3P_3Ru$ (1201.10): calcd. C 60.00, H 4.53, N 5.83; found C 60.05, H 4.58, N 5.77. IR (KBr): $\tilde{\nu}$ = 1938 cm^{-1} (ν_{CO}), 1611 ($\nu_{C=N}$), 846 (ν_{PF6}). ^1H NMR (300 MHz, $CDCl_3$, 298 K): δ = 12.99 (s, 1 H,

Table 4. Crystallographic data for **2** (Me)·CH_2Cl_2

Empirical formula	$C_{61}H_{56}Cl_2F_6N_5O_2P_3Ru$
Molecular mass	1269.99
T/K	293(2)
Crystal system	triclinic
Space group	$P\bar{1}$
a (Å)	13.437(7)
b (Å)	13.662(8)
c (Å)	16.150(9)
α (°)	77.67(5)
β (°)	86.76(4)
γ (°)	89.46(4)
V (Å^3)	2892(3)
Z	2
Calcd. density/gm^{-3}	1.459
μ (mm^{-1})	0.514
Total reflections	8598
Independent reflections	8460
R, $\omega R2[I > 2\sigma(I)]$[a][b]	0.0574, 0.1477
Goodness-of-fit on F^2 [a][b]	1.057

[a] $R_1 = \Sigma||F_o| - |F_c||/\Sigma|F_o|$. [b] $wR2 = [\Sigma w(F_o^2 - F_c^2)^2/\Sigma(F_o^2)^2$.

O−H), 10.32 (s, 1 H, 2N−H), 10.23 (s,1 H, N−H) 7.96 (s, 1 H, H7), 6.57 (s, 1 H, H5), 6.52 (s, 1 H, H3), 2.02 (s, 3 H, 21-Me), 1.84 (s, 3 H, 4-Me), 1.75 (s, 3 H, 22-Me), 3.83 (s, 3 H, OMe), 6.98−7.25 (m, 36 H, 2 PPh_3, H11, H12, H14, H15, H17, H18). Λ_M = 137 Ω^{-1} cm^{2}mol^{-1}.

2(Cl): **1**(Cl) (100 mg, 0.107 mmol) and dmbi (87 mg, 0.536 mmol) were used. Yield: 107 mg (83%). $C_{59}H_{51}ClF_6N_5O_2P_3Ru$ (1205.52): calcd. C 58.78, H 4.26, N 5.81; found C 58.82, H 4.29, N 5.76. IR (KBr): $\tilde{\nu}$ = 1940 cm^{-1} (ν_{CO}), 1605 ($\nu_{C=N}$), 848 (ν_{PF6}). ^{1}H NMR (300 MHz, $CDCl_3$, 298 K): δ = 12.69 (s, 1 H, O-H), 10.19 (s, 1 H, N−H), 10.09 (s, 1 H, N−H), 7.95 (s, 1 H, H7), 6.62 (s, 1 H, H5), 6.54 (s, 1 H, H3), 2.02 (s, 3 H, 21-Me), 1.83 (s, 3 H, 4-Me), 1.75 (s, 3 H, 22-Me), 6.90−7.34 (m, 36 H, 2 PPh_3, H11, H12, H14, H15, H17, H18). Λ_M = 138 Ω^{-1} cm^2 mol^{-1}.

X-ray Crystallography: Bright yellow single crystals of [Ru(η^1-MeL)$(PPh_3)_2$(CO)(dmbi)](PF_6)·CH_2Cl_2 (2(Me)·CH_2Cl_2) (0.40 × 0.30 × 0.25 mm^3) were grown by slow diffusion of hexane into dichloromethane solutions at room temperature. Cell parameters were determined by a least-squares fit of 30 machine-centered reflections (2θ range 14−28°) on a Siemens R3m/V four-circle diffractometer with graphite-monochromated Mo-K_α radiation (λ = 0.71073). Two check reflections measured after every 198 reflections showed no significant intensity reduction. All data were corrected for Lorentz polarization effects and an empirical absorption correction[39] was performed on the basis of an azimuthal scan of six reflections for the crystals. The metal atom was located from Patterson maps and the rest of the non-hydrogen atoms and all the hydrogen atoms except those of CH_2Cl_2 emerged from successive Fourier syntheses. The structure was refined by a full-matrix least-squares procedure. All non-hydrogen atoms were refined anisotropically. The hydrogen atoms were refined isotropically with a fixed *U* = 0.08 Å^2. Calculations were performed using the SHELXTL, version 5.03[40] package. Crystal data are listed in Table 4. CCDC-210733 contains the supplementary crystallographic data for **2** (Me)·CH_2Cl_2. These data can be obtained free of charge at www.ccdc.cam.ac.uk/conts/retrieving.html [or from the Cambridge Crystallographic Data Centre, 12, Union Road, Cambridge CB2 1EZ, UK; Fax: (internat.) +44-1223-336-033; E-mail: deposit@ccdc.cam.ac.uk].

Computer Generation of Motif 5: The relative positions of CO and the dmbi chelate were retained as in the structure of [Ru(η^1-MeL)$(PPh_3)_2$(CO)(dmbi)](PF_6)·CH_2Cl_2 but the phenolic oxygen O(1) was shifted so as to correspond to the relative position in **1** (Me), the C−O length being set at 1.347(6) Å. The same software as noted above was used.

Acknowledgments

We are thankful to the Department of Science and Technology, the Council of Scientific and Industrial Research, New Delhi, India, for financial support. The help received from Professor M. Choudhury, Dr. S. Goswami, and Dr. D. Nath is acknowledged.

[1] M. Poyatos, J. A. Mata, E. Falomir, R. H. Crabtree, E. Peris, *Organometallics* **2003**, *22*, 1110−1114.
[2] J. Perez, V. Riera, A. Rodriguez, D. Miguel, *Organometallics* **2002**, *21*, 5437−5438.
[3] J. A. Cabeza, I. D. Rio, S. G. Granda, V. Riera, M. Suarez, *Organometallics* **2002**, *21*, 2540−2543.
[4] W. Ferstl, I. K. Sakodinskaya, N. B. Sutter, G. L. Borgne, M. Pfeffer, A. D. Ryabov, *Organometallics* **1997**, *16*, 411−418.
[5] K. Ghosh, S. Pattanayak, A. Chakravorty, *Organometallics* **1998**, *17*, 1956−1960.
[6] K. Ghosh, S. Chattopadhyay, S. Pattanayak, A. Chakravorty, *Organometallics* **2001**, *20*, 1419−1423.
[7] P. Steenwinkel, S. L. James, R. A. Gossage, D. M. Grove, H. Kooijman, W. J. J. Smeets, A. L. Spek, G. V. Koten, *Organometallics* **1998**, *17*, 4680−4693.
[8] B. K. Panda, S. Chattopadhyay, K. Ghosh, A. Chakravorty, *Organometallics* **2002**, *21*, 2773−2780.
[9] V. Ritleng, M. Pfeffer, C. Sirlin, *Organometallics* **2003**, *22*, 347−354.
[10] V. W. W. Yam, B. W. K. Chu, K. K. Cheung, *Chem. Commun.* **1998**, 2261−2262.
[11] V. W. W. Yam, B. W. K. Chu, C. C. Ko, K. K. Cheung, *J. Chem. Soc., Dalton Trans.* **2001**, 1911−1919.
[12] P. Ghosh, N. Bag, A. Chakravorty, *Organometallics* **1996**, *15*, 3042−3047.
[13] N. Bag, S. B. Choudhury, A. Pramanik, G. K. Lahiri, A. Chakravorty, *Inorg. Chem.* **1990**, *29*, 5013−5014.
[14] N. Bag, S. B. Choudhury, G. K. Lahiri, A. Chakravorty, *J. Chem. Soc., Chem. Commun.* **1990**, 1626−1627.
[15] S. Chattopadhyay, K. Ghosh, S. Pattanayak, A. Chakravorty, *J. Chem. Soc., Dalton Trans.* **2001**, 1259−1265.
[16] S. Chattopadhyay, K. Ghosh, S. Pattanayak, A. Chakravorty, *Indian J. Chem.* **2001**, 40A, 1−3.
[17] P. Ghosh, A. Pramanik, A. Chakravorty, *Organometallics* **1996**, *15*, 4147−4152.
[18] P. Ghosh, A. Chakravorty, *Inorg. Chem.* **1997**, *36*, 64−69.
[19] S. Chattopadhyay, B. K. Panda, K. Ghosh, A. Chakravorty, *Israel J. Chem.* **2001**, *41*, 139−144.
[20] B. K. Panda, S. Chattopadhyay, K. Ghosh, A. Chakravorty, *Polyhedron* **2002**, *21*, 899−904.
[21] D. P. Rillema, R. Sahai, P. Matthews, A. K. Edwards, R. J. Shaver, L. Morgan, *Inorg. Chem.* **1990**, *29*, 167−175.
[22] M. Haga, M. M. Ali, H. Maegawa, K. Nozaki, A. Yoshimura, T. Ohno, *Coord. Chem. Rev.* **1994**, *132*, 99−104.
[23] M. Haga, M. M. Ali, S. Koseki, K. Fujimoto, A. Yoshimura, K. Nozaki, T. Ohno, K. Nakajima, D. J. Stufkens, *Inorg. Chem.* **1996**, *35*, 3335−3347.
[24] M. Haga, T. Inoue, S. Yamabe, *Inorg. Chem.* **1987**, *26*, 4148−4154.
[25] P. Majumdar, S. M. Peng, S. Goswami, *J. Chem. Soc., Dalton Trans.* **1998**, 1569−1574.
[26] C. Sandorfy, D. Vocelle, *Mol. Phys. Chem. Biol.* **1989**, 4, 195−211.
[27] H. Bohme, M. Hakke, in *Advances in Organic Chemistry* (H. Bohme, H. G. Viehe, Eds.), Part 1, Vol. 9, Interscience Publication, New York, **1976**, p.1.

[28] N. Serpone, D. G. Bickley, *Inorg. Chem.* **1972**, *17*, 391−397.
[29] P. Ghosh, *Polyhedron* **1997**, *16*, 1343−1349.
[30] A. K. Rappe, C. J. Caswit, K. Colwell, W. A. Goddard, W. M. Skiff, *J. Am. Chem. Soc.* **1992**, *114*, 10024−10035.
[31] J. E. Huheey, E. A. Keiter, R. L. Keiter, *Inorganic Chemistry: Principles of Structure and Reactivity*, Hampen Collins College Publishers, New York, **1993**, p. 292.
[32] F. Grepioni, G. Cojazzi, S. M. Drapen, N. Scully, D. Braga, *Organometallics* **1998**, *17*, 296−307.
[33] D. P. Rillema, D. G. Taghdiri, D. S. Jones, L. A. Worl, T. J. Meyer, H. A. Levy, C. D. Keller, *Inorg. Chem.* **1987**, *26*, 578−585.
[34] M. Haga, *Inorg. Chim. Acta* **1983**, *77*, L39−L41.
[35] G. K. Lahiri, S. Bhattacharya, B. K. Ghosh, A. Chakravorty, *Inorg. Chem.* **1987**, *26*, 4324−4331.
[36] P. Ghosh, A. Pramanik, N. Bag, G. K. Lahiri, A. Chakravorty, *J. Organomet. Chem.* **1993**, *454*, 237−241.
[37] T. A. Stephenson, G. Wilkinson, *J. Inorg. Nucl. Chem.* **1966**, *28*, 945−956.
[38] A. Pramanik, N. Bag, D. Ray, G. K. Lahiri, A. Chakravorty, *Inorg. Chem.* **1991**, *30*, 410−417.
[39] A. C. T. North, D. C. Phillips, F. A. Mathews, *Acta Crystallogr., Sect. A* **1968**, 24, 351−359.
[40] G. M. Sheldrick, SHELXTL, Version 5.03; *Siemens Analytical X-ray system:* Madison, WI, **1994**.

Received May 17, 2003
Early View Article
Published Online October 31, 2003

